Available online at www.sciencedirect.com
SCIENCE DIRECT®
Journal of Solid State Chemistry 171 (2003) 12–18
JOURNAL OF SOLID STATE CHEMISTRY
http://elsevier.com/locate/jssc

Structure, particle size, and annealing of gas phase-condensed Eu^{3+}:Y_2O_3 nanophosphors

B.M. Tissue* and H.B. Yuan[1]

Department of Chemistry, Virginia Polytechnic Institute and State University, Blacksburg, VA 24061-0212, USA

Received 2 May 2002; received in revised form 1 August 2002

Abstract

This paper reports the phase distribution and particle size of Eu^{3+}:Y_2O_3 nanoparticles prepared by gas-phase condensation as a function of preparation conditions and annealing. Annealing improves the crystallinity of the as-prepared nanoparticles but also increases the particle size. Gas-phase condensation at a low pressure (10 Torr) produces 5-nm Eu^{3+}:Y_2O_3 in multiple phases. Annealing the 5-nm nanoparticles produces single-phase material in the cubic structure with a doubling of the particle size. Higher chamber pressures produce larger particles. A pressure of 400 Torr produces 13-nm Eu^{3+}:Y_2O_3 in the monoclinic structure. Annealing the 13-nm particles produces a mixture of monoclinic and cubic phase material with a 50% increase in average particle size. We also report preliminary attempts to disperse Eu^{3+}:Y_2O_3 and Eu_2O_3 nanoparticles in different surfactant and polymer solutions.

Keywords: Nanoparticle; Europium; Yttria; Luminescence; Sintering; Size dependence; Metastable phase

1. Introduction

Europium-doped Y_2O_3 is a common red phosphor in lighting and display applications [1], and nanoscale Eu^{3+}:Y_2O_3 is a candidate for new applications in field-emissive displays (FED) and high-definition television (HDTV) [2–4]. Producing optical materials in nanoscale forms opens new opportunities to create materials with new or enhanced properties and to use polycrystalline materials in new applications [5,6]. However, creating nanoscale optical materials can also introduce detrimental effects due to changes in the structural and optical properties. Structurally, forming materials in nanoscale can produce metastable crystal structures [7], and affect the degree of inhomogeneous distortion and dopant distribution [8,9]. The optical properties of a luminescent ion in a nanoscale host can change due to changes in the band edge or charge-transfer bands [10,11], and due to changes in the phonon spectrum, phonon relaxation, or the electron–phonon interaction [12–14], The spontaneous transition rate can depend on the nanoparticle surroundings [15], and the high surface-to-volume ratio can lead to greater quenching due to surface defects [16].

Nanoparticles and nanostructured films of doped and undoped Y_2O_3 have been synthesized by a variety of methods [2,4,11,17], In many of these methods, the as-prepared material is annealed to attain a preferred phase and to improve the crystallinity for the highest luminescence efficiency [10,16]. Annealing usually results in an increased particle size. Grain growth can be suppressed using appropriate dopants [18], and recently a two-step sintering process produced a full-density nanostructured yttria ceramic without late-stage grain growth [19]. Many phosphor applications can be met with particles on the scale of tens or hundreds of nanometers, however, new types of applications such as bioimaging can require smaller particles [20]. In this paper we investigate the annealing effects on Eu^{3+}:Y_2O_3 nanoparticles produced by inert-gas condensation, which allows us to study Y_2O_3 particles in the 4–20 nm range [21,22]. Past studies using this preparation method have shown metastable phases [7], lifetime dependence on the surroundings [15], and phonon restriction effects (in Eu_2O_3) [17]. We have not made measurements of

*Corresponding author. Fax: 540-231-3255.
E-mail address: tissue@vt.edu (B.M. Tissue).
[1]Current address: AXT-LED Technologies, Monterey Park, CA 91754, USA.

0022-4596/03/$ - see front matter © 2002 Elsevier Science (USA). All rights reserved.
doi:10.1016/S0022-4596(02)00140-8

band edge changes or quantum efficiencies in our samples.

2. Experimental section

The nanoparticles were prepared by inert-gas condensation using a CO_2 laser to heat a spot of approximately 1-mm diameter on a ceramic target [22]. The target was a sintered pellet of 0.1% Eu^{3+}:Y_2O_3 that rotated on a platform in a vacuum chamber. In this study, the condensation chamber was filled with 10 or 400 Torr of nitrogen to prepare smaller or larger particles, respectively. The nanoparticles collected on a stainless steel cone approximately 3.5 cm directly above the heated spot. The nanoparticles thus made are labeled 'as-prepared'. Portions of the nanoparticles were annealed as loose powders in platinum crucibles in a box furnace. The dopant concentration is taken to be the same as the target, although some enrichment of europium is common. There was no evidence in the optical spectra or transients of the annealed samples to indicate a significantly higher average concentration [7].

The particle morphology and average particle diameter were obtained from transmission electron micrographs using a Philips EM 420 scanning transmission electron microscope (TEM) operated at 100 kV. The crystal structure was confirmed by powder X-ray diffraction (XRD) using a Scintag XDS 2000 diffractometer with Cu$K\alpha$ radiation. For optical spectroscopy, the nanoparticle powders were packed into a depression on a copper sample holder and mounted on the cold head of a cryogenic refrigerator (Cryomech GB15). The sample was maintained at approximately 12 K for all spectroscopic measurements. The excitation source was a Nd^{3+}:YAG-pumped dye laser (Continuum) with Coumarin 540A dye (Exciton). Excitation and luminescence spectra were obtained using a 6-nm bandpass, 0.25-m monochromator with a Hamamatsu P-28 PMT or a 0.3-nm bandpass, 1-m monochromator (Spex 1000 M) with Hamamatsu R-636 GaAs PMT. Spectra were recorded with a gated photon counter (Stanford SR400) and computer data acquisition. Luminescence decay transients were recorded by signal averaging with a 350-MHz digital oscilloscope (Tektronix TDS460).

3. Results

3.1. Five-nanometer Eu^{3+}:Y_2O_3 (condensation at 10 Torr)

3.1.1. Five-nanometer Eu^{3+}:Y_2O_3 as-prepared

Fig. 1(a) shows a TEM micrograph of the as-prepared nanoparticles synthesized in a 10-Torr nitrogen atmosphere. The networked morphology is typical for gas-phase-condensed nanoparticles. The average diameter measured by TEM of these as-prepared particles is approximately 5 nm (4.7 nm calculated average) with a 95% distribution within ± 1 nm. Fig. 2(a) shows the particle size distribution as determined by surveying micrographs. The powder XRD pattern of this sample (not shown) contains a strong background and several broad reflections. The XRD lines are not well resolved, but close to those of both the cubic and monoclinic phase.

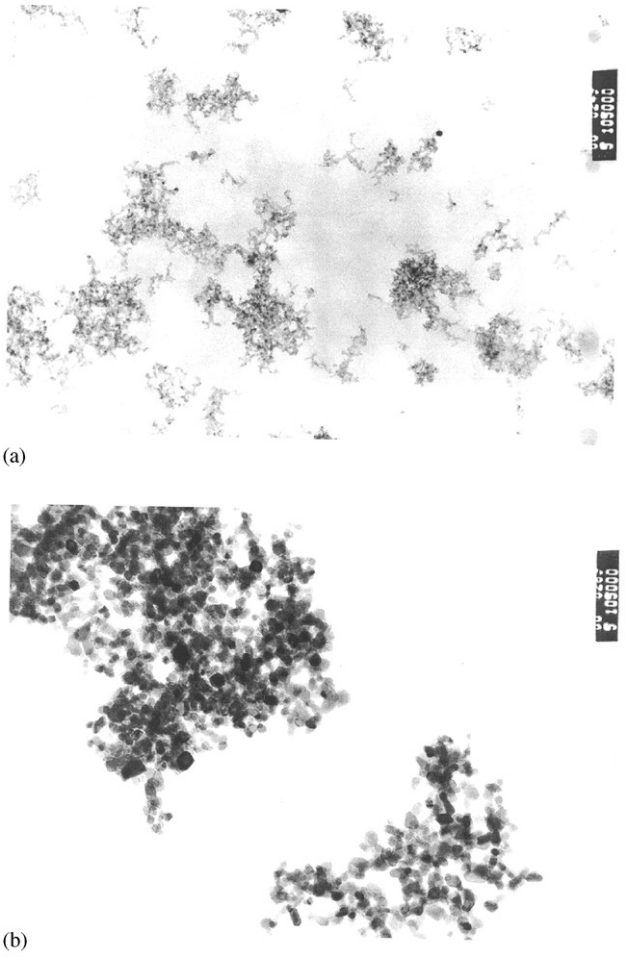

Fig. 1. (a) TEM micrograph of as-prepared 0.1% Eu^{3+}:Y_2O_3 nanoparticles prepared in 10 Torr N_2. (b) The same nanoparticle sample annealed at 800°C for 24 h. The magnification of these positive micrographs is 210 000.

Fig. 3 shows the $^7F_0 \rightarrow {}^5D_0$ excitation spectrum of the as-prepared nanoparticles monitoring $^5D_0 \rightarrow {}^7F_2$ luminescence at 614.7 nm, where several phases have overlapping emission lines. The spectrum shows that Eu^{3+} is present in this as-prepared sample in multiple phases: monoclinic Y_2O_3, cubic Y_2O_3, monoclinic Eu_2O_3, and an unknown phase that produces a very broad band. In general, the optical spectra of lanthanides can provide greater sensitivity than XRD to detect secondary phases. The monoclinic structure has three distinct crystallographic sites, labeled *A*, *B*, and *C*. The cubic structure

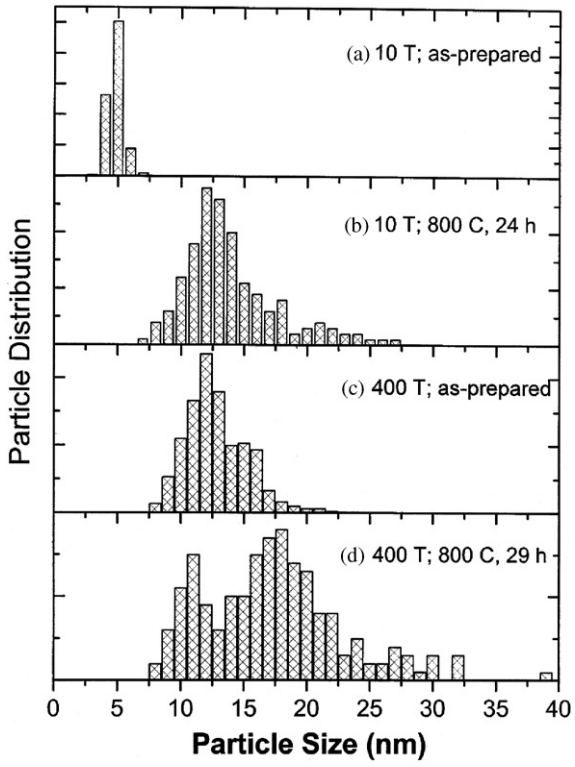

Fig. 2. Particle size distribution of 0.1% Eu^{3+}:Y_2O_3 nanoparticles as determined from a survey of TEM micrographs. Inert-gas pressure during gas-phase condensation and annealing are indicated in the figure.

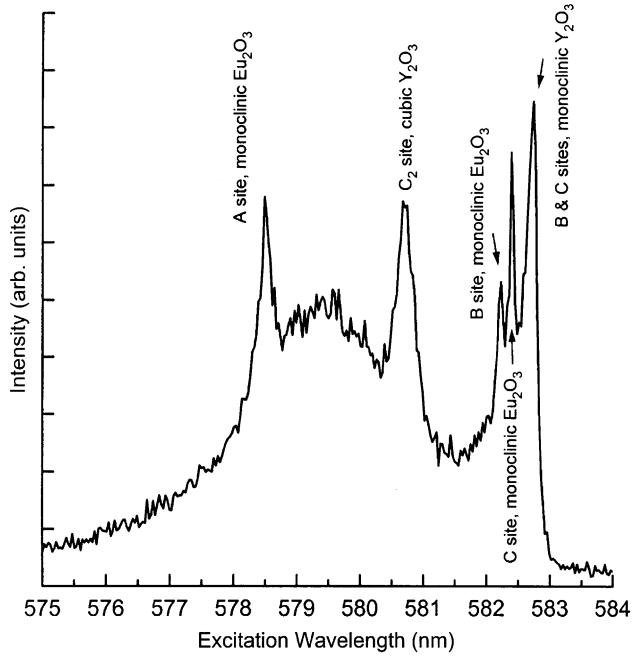

Fig. 3. Excitation spectrum of 0.1% Eu^{3+}:Y_2O_3 nanoparticles as-prepared at 10 Torr. $^5D_0 \rightarrow {}^7F_2$ luminescence was monitored at 614.7 nm with a bandpass of 0.3 nm.

has two sites, but only the stronger C_2 site is visible in this spectrum. The assignment of the excitation lines was confirmed by exciting each peak in the spectra and

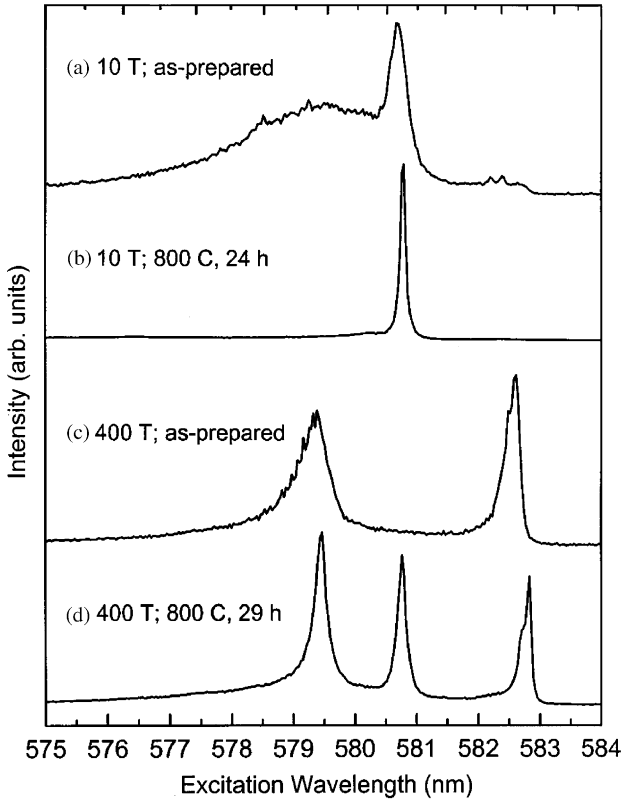

Fig. 4. Broad-band excitation spectra of as-prepared and annealed 0.1% Eu^{3+}:Y_2O_3 nanoparticles. $^5D_0 \rightarrow {}^7F_2$ luminescence was monitored at 612 nm with a bandpass of 6 nm to include all phases.

comparing the resulting luminescence spectra (not shown) to previous samples [7,23,24]. The broad band centered at approximately 579.5 nm is attributed to a very disordered phase of indeterminate crystal structure, which is consistent with the background observed in the XRD pattern. The Fig. 3 spectrum is recorded by monitoring $^5D_0 \rightarrow {}^7F_2$ luminescence at 615 nm to enhance the signal from Eu^{3+} in the monoclinic phases. The fraction of nanoparticles in the monoclinic phases is relatively small compared to the disordered phase and the cubic phase. Fig. 4(a) shows the excitation spectrum of this sample monitoring $^5D_0 \rightarrow F_2$ luminescence at 612 nm to enhance the cubic phase line.

3.1.2. Five-nanometer Eu^{3+}:Y_2O_3 annealed at different temperatures

The as-prepared, 5-nm nanoparticles were divided into several portions and each portion was annealed in air for 24 h at a temperature between 300°C and 900°C. Fig. 5 shows the average particle size obtained from TEM micrographs versus the annealing temperature. The particle size becomes significantly larger for annealing temperatures greater than approximately 600°C. Fig. 2(b) shows the resulting particle distribution for the 5-nm sample annealed at 800°C and Fig. 4(b) also shows the resulting excitation spectrum. Fig. 6

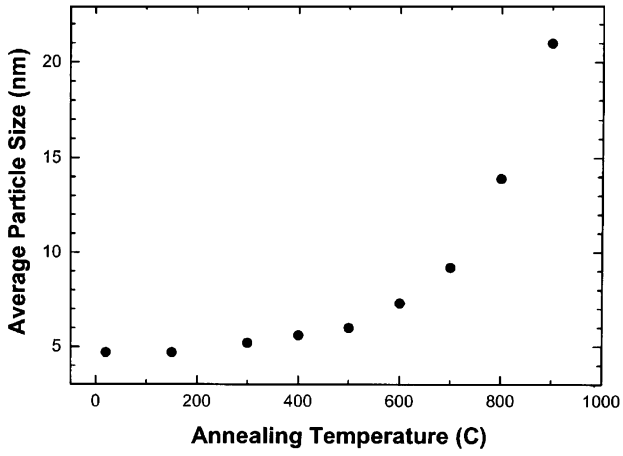

Fig. 5. Average particle diameters of 0.1% Eu^{3+}:Y_2O_3 nanoparticles annealed in air for 24 h.

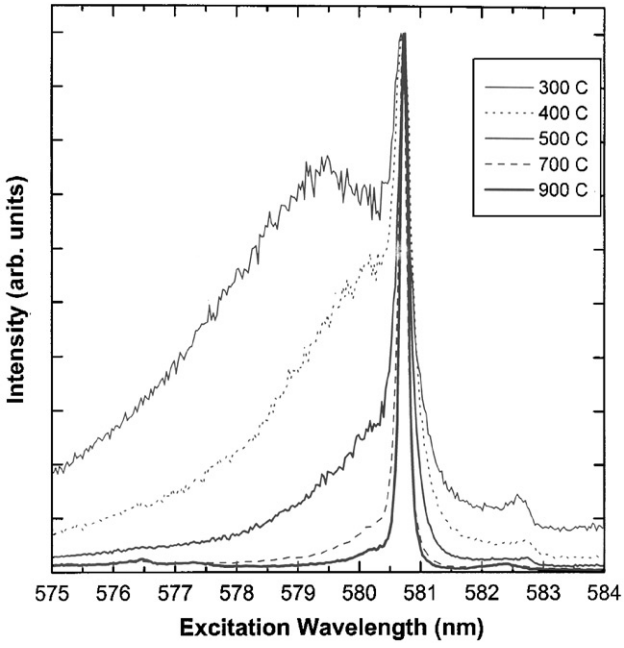

Fig. 6. Broad-band excitation spectra of 0.1% Eu^{3+}:Y_2O_3 nanoparticles annealed at various temperatures for 24 h. $^5D_0 \rightarrow {}^7F_2$ luminescence was monitored at 612 nm with a bandpass of 6 nm to include all phases. All spectra are normalized to the maximum intensity.

shows a more detailed study of the excitation spectrum as a function of temperature. As the annealing temperature increases, the emission from the cubic phase of Eu^{3+}:Y_2O_3 grows and the emission is essentially eliminated from the other phases at 700°C and higher. XRD results (not shown) also confirm that the sample can be converted to the cubic-phase completely. The overall luminescence intensity does not change significantly, but it is concentrated in the cubic-phase emission. The cubic-phase luminescence of the sample annealed at 900°C increased by approximately two orders of magnitude compared to the as-prepared material. The luminescence lifetime provides a check on the phase purity and dopant distribution. In samples annealed above 600°C, the luminescence decay of the cubic phase is a single exponential function of time. The luminescence lifetime remains ~3 ms when the nanoparticles are not packed under high pressures [15]. Annealing the nanoparticles at less than 600°C produces a more complicated luminescence decay which is not single exponential. Presumably, overlap of lines from the multiple structural phases results in a summation of decay transients that have different lifetimes. It is also possible that there is energy transfer between different phases, but we have not investigated this possibility in detail.

3.1.3. *Five-nanometer Eu^{3+}:Y_2O_3 annealed at 800°C*

In another series of annealing experiments, the as-prepared, 5-nm nanoparticles were annealed at 800°C for 15 min, 1,4, and 24 h. Fig. 7 shows the average particle size versus annealing time. (Note that the average size tends to be slightly higher than the peak in the particle size distribution in Fig. 2.) The nanoparticle grain growth is very fast initially and then slows with time. Annealing at 800°C for a period as short as 15 min also greatly reduces the luminescence from the disordered phase and the Eu_2O_3 and Eu^{3+}:Y_2O_3 monoclinic phases. Annealing at 800°C for 15 min produced the same results in TEM and spectroscopy as annealing at 700°C for 24 h (see the 700°C spectrum in Fig. 6).

3.2. *Thirteen-nanometer Eu^{3+}:Y_2O_3 (400-Torr)*

Nanoparticles prepared with a chamber atmosphere of 400-Torr nitrogen have an average size of 13 nm. Fig. 2(c) shows the particle size distribution for this as-prepared material. The excitation spectrum in Fig. 3(c), fluorescence spectra, and XRD show only

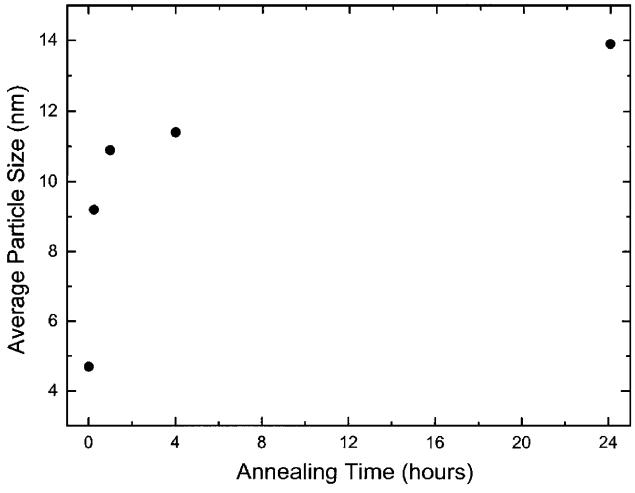

Fig. 7. Average particle diameters of 0.1% Eu^{3+}:Y_2O_3 nanoparticles annealed at 800°C in air for 15 min, 1,4, and 24 h.

the Eu^{3+}:Y_2O_3 monoclinic phase for 13-nm, as-prepared nanoparticles. Annealing the as-prepared, 13-nm nanoparticles at 800°C for 24 h increases the particle size and the size distribution (see Fig. 2(d)) but mostly retains the monoclinic phase. The excitation spectrum in Fig. 4(d) shows that both the monoclinic and cubic phases are present. The total intensity from the monoclinic phase is approximately 3 time higher than that from the cubic phase, even when the luminescence wavelength was monitored at 612 nm to favor the cubic phase. No significant changes were observed in this sample after annealing at 1000°C for an additional 24 h.

4. Annealing discussion

The magnitude of the grain growth on annealing that we observe is comparable to other reports [16,10,25]. Annealing the 5-nm particles at 800°C eliminated the secondary phases and produced single-phase material in the cubic structure in a very short time. The rapid change on annealing, including the disappearance of the broad band in the excitation spectrum, suggests that an unstable amorphous phase is present in the smallest as-prepared samples. Whether the different phases arise from separate discreet particles or multiphase particles, e.g., surface and interior phases, is not determined. Annealing the 13-nm, as-prepared nanoparticles increases the particle size and the size distribution, and mostly retains the monoclinic structure with some cubic phase material detected. The as-prepared, 5- and 13-nm nanoparticles thus show a significantly different annealing behavior.

In micrometer-sized Y_2O_3, the cubic phase is the stable structure at ambient conditions. The monoclinic phase is metastable and can be obtained only by quenching Y_2O_3 powders from high temperature and under high pressure [26]. Formation of the monoclinic structure in Y_2O_3 nanoparticles has been attributed to the Gibbs–Thomson effect, in which the increased surface tension converts the particle to the denser metastable phase [21]. If this was the only effect controlling the nanoparticle crystal structure, then it would be an even larger factor in the 5-nm particles. However, the 5-nm particles are predominantly in the cubic and disordered phases with annealing producing only the cubic phase, so other factors must play significant roles in the resulting structure. A variety of preparation and annealing procedures have produced nanoparticles in this size range in the cubic phase [8–10,16,25], and one study produced the cubic structure for 20-nm particles and the monoclinic structure for 10-nm particles [27]. The stable phase appears to depend on the details of sample preparation and annealing, and not only on the particle size alone. In our samples, the TEM micrographs show that the nanoparticles are not spherical and the faceting could influence the structure [28]. The presence of necks between particles [21], annealing loose versus compacted powders, and the presence of adsorbates and the detailed surface chemistry can also play a significant role [29]. The particle size distribution in Fig. 2(d) hints at a bimodal distribution. A possible explanation for the existence of both monoclinic and cubic phases in the annealed 13-nm sample is that the initial particle size distribution spans a critical particle size, as reported in annealing studies of other nanoscale materials [30–32].

5. Dispersing nanoparticles in solution

The TEM micrographs show that the as-prepared and annealed nanoparticles are "connected" by necks. Having mono-dispersed nanoparticles in solution is necessary for many applications and for further processing or assembly of nanocomposites. To investigate if the gas-phase-condensed nanoparticles are sintered together tightly, we did some preliminary experiments to disperse oxide nanoparticles in various solutions containing surfactants and polymers. Due to the availability of material, these dispersion experiments used a variety of nanoparticles prepared by gas-phase condensation: Eu_2O_3 nanoparticles dried at 100°C, Eu_2O_3 nanoparticles annealed at 800°C for 24 h, and 5% Eu^{3+}:Y_2O_3 nanoparticles annealed at 800°C for 24 h. The nanoparticles in the different solutions were held in an ultrasonic bath for 30 min or longer. All experiments were at room temperature unless noted. The extent of the dispersion was monitored by the transparency of the solutions and by TEM. When preparing samples for TEM, the copper grids were dipped into the sample solutions and then dried in air.

5.1. AOT surfactant

A solution of 0.1 M AOT (AOT = dioctyl sulfosuccinate sodium salt) in hexane was transparent without nanoparticles. Adding annealed nanoparticles (4 mg of Eu_2O_3 or Eu^{3+}:Y_2O_3 into 4 mL of solution) followed by ultrasonic treatment produced a turbid, white suspension. After discontinuing the ultrasound, approximately one-half of the nanoparticles settled to the bottom of the container within one hour. There was no observable change in the solution after standing overnight.

5.2. $C_{12}TAB$ surfactant

A solution of 0.05 M $C_{12}TAB$ ($C_{12}TAB$ = dodecyl trimethyl ammonium bromide) in methanol was transparent before adding in nanoparticles. Adding several mg of dried Eu_2O_3 nanoparticles into 4 mL of solution and ultrasonicating produced a white suspension. Most

of the nanoparticles settled to the bottom of the container in 2 h. A small amount of nanoparticles remained in the transparent part of the solution as detected a very weak luminescence on optical excitation.

5.3. Polybutadiene

Twenty-two mg of annealed Eu_2O_3 nanoparticles were added to 20 mL of hexane followed by 2 min in the ultrasonic bath. The solution was very turbid with a white color. Sixty milligrams of chopped polybutadiene grains were then added and the solution was heated to 70°C for 15 min. The polymer grains dissolved completely and the solution remained turbid. After 2 h in the ultrasonic bath the solution became much lighter in color and less turbid. The suspension was stable, no precipitation was observed after letting the solution stand overnight. Reversing the order of addition of the nanoparticles and polymer to the hexane produced the same results. The white color indicates scattering by agglomerates that are larger than the visible light wavelengths, so apparently the polymer stabilizes the nanoparticle agglomerates but does not produce a monodisperse solution.

5.4. Polystyrene

Forty milligrams mg of polystyrene was dissolved in 5 mL of CS_2 at 75°C. After the solution cooled to room temperature, it turned from transparent to light blue. Three milligrams of annealed Eu_2O_3 nanoparticles were added to this solution. The nanoparticles remained in relatively large flocs, which were visible by eye, even after heating and ultrasonic treatment.

5.5. AOT surfactant and polybutadiene

1.8 mg AOT was added to 20 mL hexane and stirred until it became transparent. Adding 10 mg of annealed Eu_2O_3 nanoparticles caused the solution to become turbid. After keeping the solution in the ultrasonic bath for 15 min, 120 mg of polybutadiene was added. The solution was heated to 75°C to dissolve the polymer and then ultrasonicated for 2 h. On standing overnight the solution became almost transparent with a very light blue color. Since this procedure gave the best visual results, it was checked by TEM. The TEM micrographs showed nanoparticles in groups of 10–30 nanoparticles. No isolated nanoparticles or groups of >100 particles were observed. The absence of single nanoparticles could be an artifact of sample preparation since the drying procedure could bring nanoparticles together.

5.6. Dilute HCl

A dilute acid solution with a pH of approximately 5 was prepared by diluting HCl with de-ionized water. Three milligrams of annealed Eu_2O_3 nanoparticles were added to 3 mL of this solution and then placed in the ultrasonic bath for 30 min. The resulting solution was homogeneous with no precipitation and a very light blue color. Visually, this solution was comparable to the dispersion using AOT and polybutadiene. TEM micrographs showed that the nanoparticles were mostly in small groups, typically of 5–20 particles, however, groups of approximately 100 nanoparticles were also observed. All of the dispersion results are summarized in Table 1. Using only surfactant or polymer did not produce monodispersed nanoparticles. Using both AOT surfactant and polybutadiene produced the best results and was similar to a slightly acidic aqueous solution.

5.7. Eu_2O_3 embedded in polymer

Eu_2O_3 nanoparticles were embedded in polybutadiene by filling a 5-mm mold with the polymer/nanoparticle suspension and allowing the hexane to evaporate. The sample displayed a significant intensity of luminescence

Table 1
Summary of dispersion experiments

Surfactant/polymer	Solvent	Nanoparticle(s), annealing temperature	Result
0.1 M AOT	Hexane (4 mL)	Eu_2O_3 or Eu:Y_2O_3 , 800°C (4 mg)	Partially settled
0.05 M C_{12}TAB	Methanol	Eu_2O_3, 100°C	Settled
Poly butadiene (60 mg)	Hexane (20 mL)	Eu_2O_3, 800°C (22 mg)	White suspension
Poly styrene (40 mg)	CS_2 (5 mL)	Eu_2O_3, 800°C (3 mg)	White suspension
AOT (1.8 mg) and polybutadiene (120 mg)	Hexane (20 mL)	Eu_2O_3, 800°C (10 mg)	Light blue suspension
—	pH = 5 water (3 mL)	Eu_2O_3, 800°C (3 mg)	Light blue suspension

under optical excitation. Both the excitation and fluorescence spectra corresponded to monoclinic Eu_2O_3. A spectral line shift was observed when the sample temperature varied from 300 to 12 K that was not observed in the Eu_2O_3 nanoparticles alone. The cause of this shift is not known but must be associated with the polymers in which the nanoparticles were embedded. Trying to make a thin film of Eu_2O_3 nanoparticles in polybutadiene by evaporating hexane from a AOT/polybutadiene/nanoparticle hexane solution on a glass slide produced very weak luminescence. The weak luminescence probably results from the small number of nanoparticles in the film, but attempts to prepare thicker films were not satisfactory.

6. Conclusions

Preparing gas-phase-condensed nanoparticles at 10 Torr of N_2 resulted in multiple phases with an average diameter of 5 nm. Annealing these nanoparticles at 800°C increased the particle size and transformed the structure to the cubic phase. As-prepared and annealed nanoparticles in the 12–20 nm range form in the monoclinic phase. As a result, Eu^{3+}:Y_2O_3 nanoparticles can be synthesized selectively in either cubic or monoclinic phase between 10 and 20 nm. The range of annealing results by us and others in the literature indicate that subtle factors, possibly interparticle necks, surface adsorbates, dopant concentration, etc., play a significant role in the structure after annealing. Complete monodispersion of annealed nanoparticles was not proven, however, the results indicate that the annealing does not sinter the nanoparticles to an extent that they cannot be dispersed.

Acknowledgments

The National Science Foundation supported this work under grant DMR-9871864.

References

[1] S. Shionoya, W.M. Yen, Phosphor Handbook, CRC Press, New York, 1999.
[2] A. Vecht, C. Gibbons, D. Davies, X. Jing, P. Marsh, T. Ireland, J. Silver, A. Newport, D. Barber, J. Vac. Sci. Technol. B 17 (1999) 750–757.
[3] X. Jing, T. Ireland, C. Gibbons, D.J. Barber, J. Silver, A. Vecht, G. Fern, P. Trowga, D.C. Morton, J. Electrochem. Soc. 146 (1999) 4654–4658.
[4] M.H. Lee, S.G. Oh, S.C. Yi, D.S. Seo, J.P. Hong, C.O. Kim, Y.K. Yoo, J.S. Yoo, J. Electrochem. Soc. 147 (2000) 3139–3142.
[5] C. Suryanarayana, Int. Mater. Rev. 40 (1995) 41–64.
[6] D.B. Barber, C.R. Pollock, L.L. Beecroft, C.K. Ober, Opti. Lett. 22 (1997) 1247–1249.
[7] B. Bihari, H. Eilers, B.M. Tissue, J. Lumin. 75 (1997) 1–10.
[8] T. Igarashi, M. Ihara, T. Kusunoki, K. Ohno, T. Isobe, M. Senna, Appl. Phys. Lett. 76 (2000) 1549–1551.
[9] S. Polizzi, M. Battagliarin, M. Bettinelli, A. Speghini, G. Fagherazzi, J. Mater. Chem. 12 (2002) 742–747.
[10] A. Konrad, U. Herr, R. Tidecks, F. Kummer, K. Samwer, J. Appl. Phys. 90 (2001) 3516–3523.
[11] J. Dhanaraj, R. Jagannathan, T.R.N. Kutty, C.H. Lu, J. Phys. Chem. B 105 (2001) 11098–11105.
[12] K.P. Patton, M.R. Geller, J. Lumin. 94–95 (2001) 747–750.
[13] G.K. Liu, H.Z. Zhuang, X.Y. Chen, Nano Lett. 2 (2002) 535–539.
[14] H.-S. Yang, K.S. Hong, S.P. Feofilov, B.M. Tissue, R.S. Meltzer, W.M. Dennis, J. Lumin. 83–84 (1999) 139–145.
[15] R.S. Meltzer, S.P. Feofilov, B.M. Tissue, H.B. Yuan, Phys. Rev. B 60 (1999) R14012–14015.
[16] J. McKittrick, C.F. Bacalski, G.A. Hirata, K.M. Hubbard, S.G. Pattillo, K.V. Salazar, M. Trkula, J. Am. Ceram. Soc. 83 (2000) 1241–1246.
[17] B.M. Tissue, Chem. Mater. 10 (1998) 2837–2845.
[18] C. Kleinlogel, L.J. Gauckler, Adv. Mater. 13 (2001) 1081–1085.
[19] I.-W. Chen, X.-H. Wang, Nature 404 (2000) 168–171.
[20] C.M. Niemeyer, Angew. Chem. Int. Edit. 40 (2001) 4128–4158.
[21] G. Skandan, C.M. Foster, H. Frase, M.N. Ali, J.C. Parker, H. Hahn, Nanostruct. Mater. 1 (1992) 313–322.
[22] H. Eilers, B.M. Tissue, Mater. Lett. 24 (1995) 261–265.
[23] H. Eilers, B.M. Tissue, Chem. Phys. Lett. 251 (1996) 74–78.
[24] D.K. Williams, H.B. Yuan, B.M. Tissue, J. Lumin. 83–84 (1999) 297–300.
[25] J.A. Nelson, M.J. Wagner, Chem. Mater. 14 (2002) 915–917.
[26] D.K. Williams, B. Bihari, B.M. Tissue, J.M. McHale, J. Phys. Chem. B 102 (1998) 916–920.
[27] W. Krauss, R. Birringer, Nanostruct. Mater. 9 (1997) 109–112.
[28] D.A. Jefferson, Philos. Trans. R. Soc. Lond. A 358 (2000) 2683–2692.
[29] J.M. McHale, A. Auroux, A.J. Perrotta, A. Navrotsky, Science 277 (1997) 788–791.
[30] E. Djurado, P. Bouvier, G. Lucazeau, J. Solid State Chem. 149 (2000) 399–407.
[31] H. Zhang, J.F. Banfield, J. Phys. Chem. B 104 (2000) 3481–3487.
[32] R.B. Bagwell, G.L. Messing, P.R. Howell, J. Mater. Sci. 36 (2001) 1833–1841.